Geochemistry Geophysics Geosystems

Supporting Information for

Rapid variations in fluid chemistry constrain hydrothermal phase separation at the Main Endeavour Field

Brooke Love[1], Marvin Lilley[2], David Butterfield[3], Eric Olson[2], Benjamin Larson[3]

[1] Huxley College of the Environment, Western Washington University, Bellingham, WA, USA

[2]School of Oceanography, University of Washington, Seattle, Washington, USA

[3] NOAA Pacific Marine Environmental Laboratory, Seattle, WA USA

Contents of this file

Introduction

Supporting information includes Figure S1 (a conceptual diagram illustrating the nature of changes in volatile content as fluid rises in a simplified system). Also included are Tables S1, S2 which give the uncorrected fluid chemistry data and the calculated endmember concentrations for several parameters as well as detailed information about which samples were collected at which location on the structure. Table S3 includes Fe, Mn, Mg, Si, and Cl data for geothermometer and geobarometer calculations.

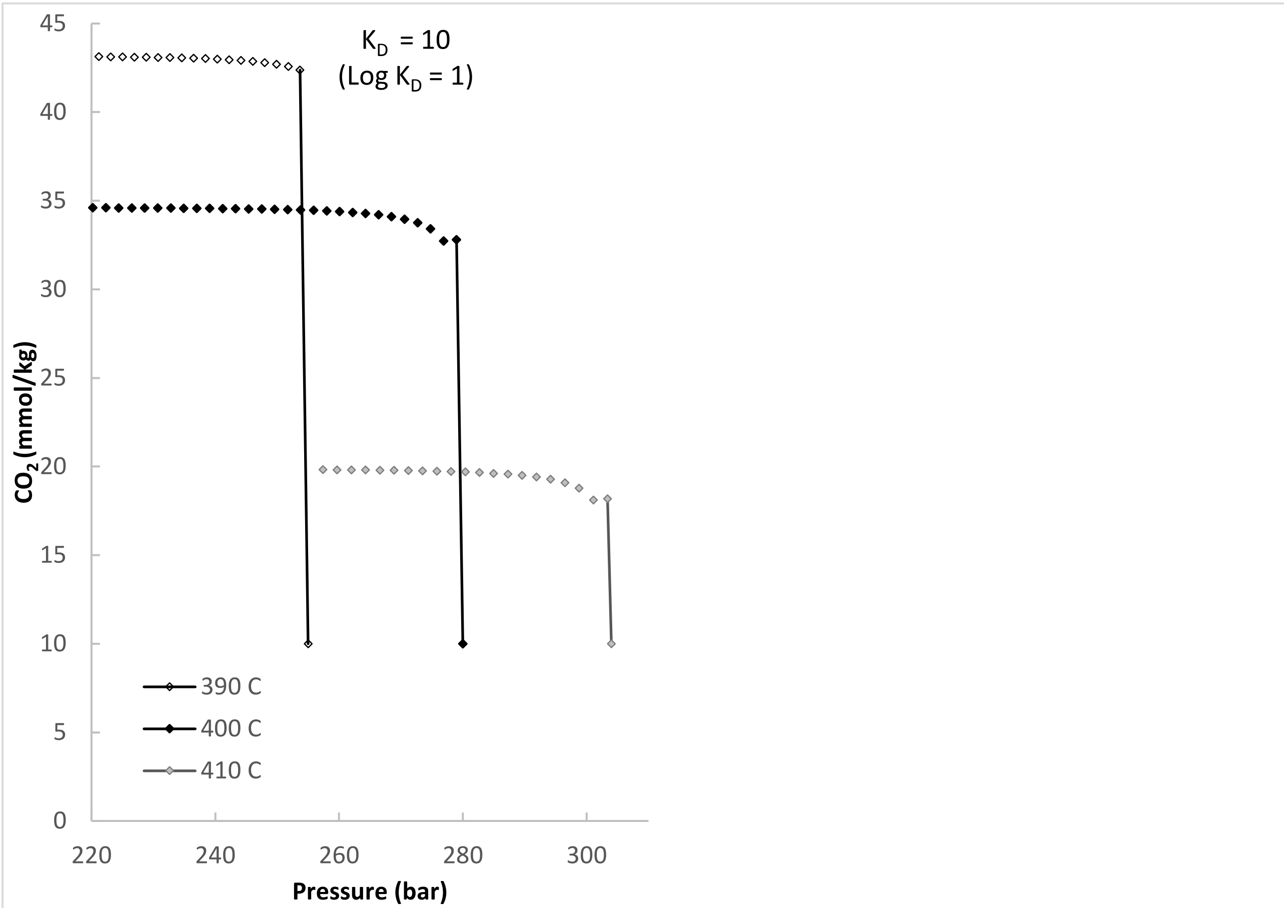

Figure S1. Simple model demonstrating the relative influence of KD, and temperature on the extent of volatile enrichment upon initial phase separation (reflected by the jump in CO2 concentration at depth) and the insensitivity of volatile concentrations to subsequent supercritical phase separation (reflected by nearly horizontal lines of CO2 vs. pressure). In this illustration, as vapor phase fluid rises, at every stage the vapor is segregated, and moves upward. No remixing with the brine is allowed and no temperature change takes place.

Table S1. Summary of primary analytical results from the Sully structure, not corrected for seawater entrainment. All concentrations are in mmol/kg. Low magnesium concentrations indicate high quality samples with minimal sea water entrainment.

Sample	Mg	Cl	H2	CH_4	CO_2	H_2S	Ar	CO
3570-10	1.84	308.77	0.379	0.941	28.65	13.55	0.016	0.0000
3577-12	2.01	318.00	0.345	0.864	27.80	12.70	0.017	0.0016
3580-15	1.35	308.80	0.436	1.047	28.12	12.84	0.017	0.0013
3582-15	5.43	333.40	0.307	0.817	27.34	9.03	0.015	0.0003
J-279-GP20	4.35	467.30	0.118	0.565	13.90	6.75	0.009	0.0086
J-279-GP22	4.26	452.50	0.127	0.563	13.66	6.29	0.009	0.0094
J-279-GP23	4.55	444.80	0.138	0.613	13.87	6.18	0.009	0.0101
J-279-GP24	3.10	456.30	0.141	0.706	13.93	6.50	0.010	0.0102
J-279-GP4	3.42	470.90	0.106	0.509	14.14	6.60	0.008	0.0076
J-279-GP-5	3.89	469.10	0.134	0.590	14.38	6.58	0.009	0.0076
J-280-12	0.31	318.20	0.208	0.680	27.50	13.37	0.009	0.0131
J-280-14	0.41	307.20	0.381	1.072	29.16	14.34	0.015	0.0072
J-280-15	0.40	304.00	0.234	0.821	32.72	16.71	0.012	0.0098
J-280-9	0.11	308.20	0.272	0.897	27.76	14.47	0.013	0.0076
3610-12	1.24	355.40	0.366	1.035	24.00	11.09	0.014	0.0153
3618-11	1.60	350.14	0.298	0.9615	23.16	11.00	0.020	0.0129
3618-GP24	8.12	372.62	0.308	0.944	19.53	7.95	0.019	0.0161
3619-8	2.51	357.07	0.358	1.037	23.08	10.17	0.016	0.0156
3621-10	2.05	359.52	0.180	0.555	17.10	8.09	0.009	0.0106

Table S2. Summary of Sully end member data from 2000, shaded areas are data from July 1st when chemistry was markedly different from the previous and subsequent samples (Fluid B). Sully Star and Star 2 were orifices located within one meter of each other near the top of the structure, and spider was located slightly lower on the structure. Star was the site of resprobe deployment. All concentrations are in mmol/kg. Italic numbers below each gas concentration represent estimated error corrected for end member extrapolation. A standard analytical error of 5% , except for 20% for CO was multiplied by a the factor: $\left({Mg_{sw}}/{(Mg_{sw} - Mg_{sample})}\right)$

Sample	Date	Temp	Cl	H_2	CH_4	CO_2	H_2S	Ar
Sully Star								
3570-10*	6/14	371	300	0.39	0.98	30	14	0.016
			15.6	*0.020*	*0.051*	*1.5*	*0.73*	*0.0008*
3577-12*	6/23	374	309	0.36	0.90	29	13	0.017
			16.1	*0.019*	*0.047*	*1.5*	*0.69*	*0.0009*
3580-15	6/26	379	302	0.45	1.07	29	13	0.017
			15.5	*0.023*	*0.055*	*1.5*	*0.68*	*0.0009*
3582-15	6/28	377	309	0.34	0.91	30	10	0.015
			17.2	*0.019*	*0.051*	*1.7*	*0.56*	*0.0008*
J-279-GP20	7/1	378	460	0.13	0.62	15	7	0.008
			25.1	*0.007*	*0.034*	*0.8*	*0.40*	*0.0004*
J-279-GP23	7/1	378	435	0.15	0.67	15	7	0.009
			23.8	*0.008*	*0.037*	*0.8*	*0.37*	*0.0005*
J-280-15	7/2	377	302	0.24	0.83	33	17	0.012
			15.2	*0.012*	*0.042*	*1.7*	*0.85*	*0.0006*
3610-12*	9/4	379	351	0.37	1.06	25	11	0.014
			18.0	*0.019*	*0.054*	*1.3*	*0.58*	*0.0007*
3618-11	9/13	377	344	0.31	0.99	24	16	0.022
			17.7	*0.016*	*0.051*	*1.2*	*0.59*	*0.0007*
3618-GP24	9/13	379	341	0.36	1.12	23	9	0.019
			20.2	*0.022*	*0.066*	*1.3*	*0.56*	*0.0011*
3619-8*	9/14	380	348	0.38	1.09	24	11	0.016
			18.3	*0.020*	*0.057*	*1.3*	*0.56*	*0.0008*
3621-10	9/16	381	352	0.19	0.58	18	8	0.006
			18.3	*0.010*	*0.030*	*0.9*	*0.44*	*0.0004*
Sully Spider								
J-279-GP4	7/1	370	466	0.11	0.54	15	7	0.008
			24.9	*0.006*	*0.029*	*0.8*	*0.38*	*0.0004*
J-279-GP-5	7/1	367	463	0.14	0.64	15	7	0.009
			25.0	*0.008*	*0.034*	*0.8*	*0.38*	*0.0005*
J-279-GP22	7/1	377	444	0.14	0.61	15	7	0.008
			24.2	*0.008*	*0.033*	*0.8*	*0.37*	*0.0005*
Sully Star 2								
J-279-GP24	7/1	377	451	0.15	0.75	15	7	0.009
			24.0	*0.008*	*0.040*	*0.8*	*0.37*	*0.0005*
J-280-12	7/2	377	317	0.21	0.68	28	13	0.009
			15.9	*0.011*	*0.034*	*1.4*	*0.68*	*0.0005*
J-280-14	7/2	377	305	0.38	1.08	29	14	0.015
			15.4	*0.019*	*0.054*	*1.5*	*0.73*	*0.0007*
J-280-9	7/2	377	308	0.27	0.90	28	14	0.013
			15.4	*0.014*	*0.045*	*1.4*	*0.73*	*0.0007*

Table S3. Uncorrected Si, Fe, and Mn and end member Si and Cl data from 2000. All concentrations are in mmol/kg except for Fe and Mn which are in µmol/kg. Temperature is in °C. Endmembers (EM) were calculated as in table S2. Some of these Si data previously presented in Fonatiane et al. (2009). Temp Fe/Mm are geothermometer estimates for equilibrium temperature with basalt based the equation of Pester et al. (2011): (°C) = 331.24 + 112.41 log[Fe/Mn].

Sample	Temp	date	Mg	Si	Fe	Mn	T Fe/Mn	Si EM	Cl EM
3570gt10	-	6/14	4.0	-	4444	898	409	-	-
3577gt12	-	6/23	15.0	-	3590	688	412	-	-
J279b11	370.3	7/1	50.3	11.9	4946	1066	406	13.1	440
J279b14	364.7	7/1	51.7	9.2	3684	809	405	11.1	374
J279b16	377.6	7/1	41.1	10.0				10.9	368
J279b17	378.5	7/1	10.7	10.7	4392	960	405	13.0	444
J279b18	378.2	7/1	51.5	9.2	3535	799	404	9.8	353
J279b19	377.7	7/1	6.3	5.2	2102	449	407	10.6	349
J279b8	370.2	7/1	52.3	11.5	4807	1034	406	12.5	434
J279b9	370.1	7/1	52.4	11.3	4537	981	406	13.8	419
J279gp20	378.2	7/1	48.3	12.0	-	-	-	13.0	461
J279gp22	177.2	7/1	41.6	12.3	-	-	-	13.3	446
J279gp23	378.1	7/1	49.1	12.2	-	-	-	13.4	436
J279gp5	367.0	7/1	49.7	12.2	-	-	-	13.8	460
3621m4		9/16	2.5	10.9	4040	907	404	11.4	371
3618b19	377.7	9/13	3.6	10.3	3650	826	404	11.1	348
3618m12	377.0	9/13	1.7	11.0	4110	882	406	11.4	367